

# Colossal magnetostriction and negative thermal expansion in the frustrated antiferromagnet $\text{ZnCr}_2\text{Se}_4$

J. Hemberger,<sup>1</sup> H.-A. Krug von Nidda,<sup>1</sup> V. Tsurkan,<sup>1,2,\*</sup> and A. Loidl<sup>1</sup>

<sup>1</sup>*Experimental Physics V, Center for Electronic Correlations and Magnetism, University of Augsburg, D-86159 Augsburg, Germany*

<sup>2</sup>*Institute of Applied Physics, Academy of Sciences of Moldova, MD-2028 Chişinău, R. Moldova*

A detailed investigation of  $\text{ZnCr}_2\text{Se}_4$  is presented which is dominated by strong ferromagnetic exchange but orders antiferromagnetically at  $T_N = 21$  K. Specific heat  $C$  and thermal expansion  $\Delta L/L$  exhibit sharp first-order anomalies at the antiferromagnetic transition.  $T_N$  is strongly reduced and shifted to lower temperatures by external magnetic fields and finally is fully suppressed suggesting a field induced quantum critical behavior close to 60 kOe.  $\Delta L/L(T)$  is unusually large and exhibits negative thermal expansion below 75 K down to  $T_N$  indicating strong frustration of the lattice. Magnetostriction  $\Delta L/L(H)$  reveals colossal values ( $0.5 \times 10^{-3}$ ) comparable to giant magnetostriction materials. Electron-spin resonance, however, shows negligible spin-orbital coupling excluding orbitally induced Jahn-Teller distortions. The obtained results point to a spin-driven origin of the structural instability at  $T_N$  explained in terms of competing ferromagnetic and antiferromagnetic exchange interactions yielding strong bond frustration.

PACS numbers: 75.30.Et, 75.40.-s, 75.50.Ee, 75.80.+q, 76.50.+g

Recently magnetic oxides and chalcogenides crystallizing in the spinel structure have attracted considerable attention. Within the last few years exotic phenomena and fascinating ground states have been observed in this class of materials: heavy-fermion behavior [1], complex spin order and spin dimerization [2, 3, 4], spin-orbital liquid [5] and orbital glass [6], as well as coexistence of ferromagnetism and ferroelectricity [7, 8]. They are attributed to the cooperativity and competition between charge, spin and orbital degrees of freedom, all of which are strongly coupled to the lattice. In addition, topological frustration due to the tetrahedral arrangement of the magnetic cations and bond frustration due to competing ferromagnetic (FM) and antiferromagnetic (AFM) exchange interactions hamper any simple spin and orbital arrangement in the ground state. Spin-lattice coupling plays an important role in releasing frustration by structural transformation. For example, in antiferromagnetic chromium-oxide spinels frustration in the spin sector due to geometrical constraints is released by a Peierls-like structural transition, which has been explained in terms of a so called spin Jahn-Teller effect [9, 10, 11]. Another source of a structural instability was recently identified in AFM  $\text{ZnCr}_2\text{S}_4$  and ascribed to competing FM and AFM exchange of nearly equal strength yielding strong bond frustration [12].

Here we present the results of a study of the spin-lattice correlations of another zinc chromium spinel,  $\text{ZnCr}_2\text{Se}_4$ , which shows an antiferromagnetic ground state despite the presence of strong FM exchange. Previous neutron-diffraction investigations revealed a complex antiferromagnetic order at temperatures below 20 K contrasting with the dominating FM interactions evidenced by a large positive Curie-Weiss temperature of 115 K [13, 14]. This testifies to the importance of the next-nearest neighbor ( $nnn$ ) exchange besides the nearest neighbor ( $nm$ ) exchange interactions [13]. The spin structure is incommensurate having a ferromagnetic arrangement in the (001) planes with a turning angle of  $42^\circ$  between the spins in the adjacent (001) planes forming a helical configura-

tion. The propagation vector of the magnetic spiral lies along one of the three equivalent  $\langle 001 \rangle$  axes [14]. The transition to the AFM state at  $T_N$  is accompanied by a structural transformation from cubic  $Fd\bar{3}m$  to tetragonal  $I4_1/amd$  symmetry with a small contraction along the  $c$  axis of  $c/a = 0.9999$  [15]. Recent neutron-diffraction and x-ray studies using synchrotron radiation more precisely defined the low temperature phase identifying an orthorhombic  $Fddd$  symmetry [16]. Such a structural transformation cannot originate from the ordinary Jahn-Teller instability, because the orbital moment of the  $\text{Cr}^{3+}$  ions is quenched in a cubic crystal field. However, as is well documented in literature, many chromium oxide and chalcogenide spinels manifest structural instabilities accompanying the magnetic ordering. In these compounds  $\text{Cr}^{3+}$  reveals a half filled  $t_{2g}$  crystal-field ground state with almost zero spin-orbit coupling. Although the oxide, sulfide, and selenide are dominated by different exchange interactions, as indicated by their Curie-Weiss (CW) temperatures, they reveal similar magnetic transition temperatures into AFM states. In  $\text{ZnCr}_2\text{O}_4$  with the smallest Cr-Cr separation and a CW temperature of -390 K, a transition from a paramagnet with strong quantum fluctuations into a planar antiferromagnet occurs at  $T_N = 12.5$  K along with a small tetragonal distortion [2, 9, 16]. The oxide is governed by strong geometrical frustration of spins coupled by direct AFM Cr-Cr exchange [17]. In sulfide,  $\text{ZnCr}_2\text{S}_4$ , with a higher Cr-Cr separation, FM Cr-S-Cr and AFM exchange interactions almost compensate each other yielding a CW temperature close to zero [12]. Below 15 K,  $\text{ZnCr}_2\text{S}_4$  undergoes a magnetic phase transition into an incommensurate helical spin order similar to that of  $\text{ZnCr}_2\text{Se}_4$  [18]. But at lower temperatures a second commensurate collinear antiferromagnetic phase develops which has a similar spin arrangement like the AFM  $\text{ZnCr}_2\text{O}_4$ . At low temperatures both magnetic phases coexist [18]. The two subsequent antiferromagnetic transitions in  $\text{ZnCr}_2\text{S}_4$  at 15 K and 8 K are accompanied by pronounced thermal and phonon anomalies. Due to strong spin-phonon coupling both mag-

netic phase transitions induce a splitting of phonon modes. The anomalies in the specific heat and thermal expansion and phonon splitting observed at 8 K are strongly suppressed by a magnetic field which supports the FM correlations. This evidences the spin-driven origin of the structural transformation related to strong competition of ferromagnetic and antiferromagnetic exchange interactions [12]. In  $\text{ZnCr}_2\text{Se}_4$ , with the highest Cr-Cr separation, the direct exchange is almost suppressed and the spin arrangement follows from the dominating FM  $mn\ 90^\circ$  Cr-Se-Cr exchange and the additional AFM  $nmn$  Cr-Se-Zn-Se-Cr and Cr-Se-Se-Cr exchange interactions [19]. Therefore, one can expect a much stronger influence of the magnetic field on the structural degree of freedom. Here we use susceptibility, electron-spin resonance (ESR), specific heat, and thermal expansion to probe the spin-lattice correlations and to elucidate the origin of the structural instability in the  $\text{ZnCr}_2\text{Se}_4$  spinel.

Polycrystalline  $\text{ZnCr}_2\text{Se}_4$  was prepared by solid-state reaction from high purity elements at 1000 °C. The single crystals were grown by chemical transport reactions between 900 and 950 °C from the polycrystalline material. X-ray diffraction analysis of the powdered single crystals at room temperature revealed a single-phase material with the cubic spinel structure (see inset in Fig. 1a) with a lattice constant  $a = 10.498(2)$  Å and a selenium fractional coordinate  $x = 0.260(1)$ . The magnetic properties were studied using a commercial SQUID magnetometer (Quantum Design MPMS-5) up to 50 kOe and a *dc* extraction magnetometer (Oxford Instruments) up to 100 kOe. The heat capacity was measured in a Quantum Design PPMS for temperatures  $2\text{ K} < T < 300\text{ K}$  and in external magnetic fields up to 70 kOe. The thermal expansion was measured employing a capacitive method in fields up to 70 kOe. The ESR studies were carried out with a Bruker ELEXSYS E500 CW-spectrometer at X-band frequency ( $\nu = 9.36\text{ GHz}$ ) in a helium gas flow cryostat (Oxford Instruments) for a temperature range between 4.2 and 300 K. For the ESR experiments a thin disk with the faces along the crystallographic (110) plane was cut from the single crystal allowing for monitoring all three principal cubic directions for the in-plane magnetic field.

Figure 1a presents the inverse susceptibility  $\chi^{-1}$  vs temperature for a single crystalline sample. For temperatures above 300 K,  $\chi$  follows a Curie-Weiss law with a positive Curie temperature  $\Theta = 90\text{ K}$  and an effective moment of  $4.04\ \mu_B$  close to the spin-only value of  $3.86\ \mu_B$  for  $\text{Cr}^{3+}$  ions in a  $3d^3$  configuration. Below 200 K,  $\chi^{-1}(T)$  deviates from the CW law indicating an increasing contribution of spin fluctuations. At 21 K the susceptibility shows a pronounced maximum with a steep drop followed by a smooth continuous decrease towards lower  $T$  (Fig. 1b). The temperature of 21 K marks the onset of long-range antiferromagnetic order at  $T_N$  identified by neutron diffraction studies [14, 16]. At temperatures below  $T_N$  the magnetization  $M$  shows a change of slope at a critical field  $H_{c1}$  of about 10 kOe characteristic for a metamagnetic transition as shown in the inset in Fig. 1b for  $T = 2\text{ K}$ . This feature corresponds to the reorientation of domains according

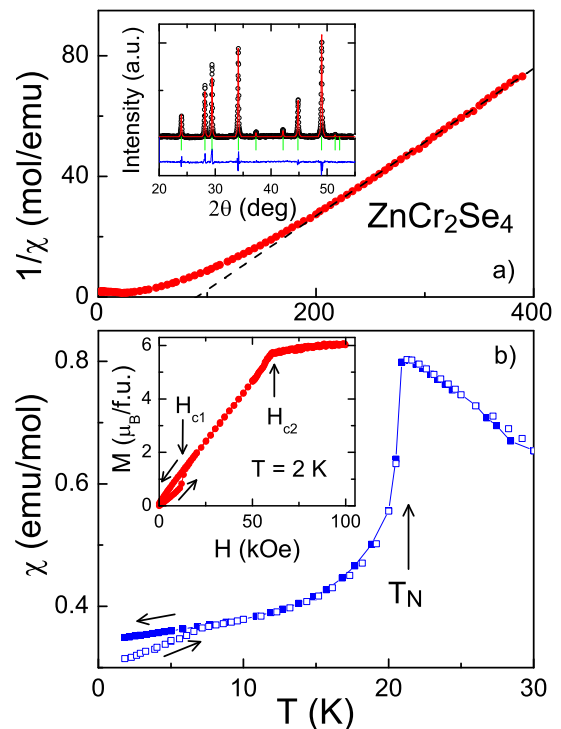


FIG. 1: (color online) a) Inverse susceptibility vs temperature as measured in a  $\text{ZnCr}_2\text{Se}_4$  single crystal at 10 kOe. The dashed line indicates a Curie-Weiss behavior. Inset: x-ray diffraction profile of the powdered single crystal. The measured intensities (open circles) are compared with the calculated profile using Rietveld refinement (solid line). Bragg positions of the normal cubic spinel structure are indicated by vertical bars and the difference pattern by the lower thin solid line; b) susceptibility vs temperature at low temperatures. The arrow indicates the magnetic phase transition at  $T_N$ . Inset: Magnetization curve for a field applied along the  $\langle 001 \rangle$  direction at 2 K. The arrows indicate the critical fields  $H_{c1}$  and  $H_{c2}$  as described in the text.

to the nearly equivalent crystallographic principal axes. The second critical field  $H_{c2}$  (which for  $T = 2\text{ K}$  is 65 kOe; see inset of Fig.1b) corresponds to the breakdown of the helical spin arrangement. Beyond  $H_{c2}$  the magnetization  $M$  reaches the full saturation of about  $3\ \mu_B$  per Cr ion.

Figure 2a shows the specific heat in the representation  $C/T$  vs  $T$  at different external magnetic fields. In the absence of a magnetic field, the specific heat manifests a sharp anomaly on approaching the Néel temperature  $T_N$ . Application of magnetic fields suppresses the peak in the specific heat concomitantly shifting it to lower temperatures. The observed peak in  $C/T$  at  $T_N$ , which is much sharper than for conventional antiferromagnets, points towards a first-order transition. The anomaly in  $C/T$  is fully suppressed by a magnetic field of 70 kOe where the helical spin arrangement is completely destroyed and the magnetization reaches the saturation as discussed above. The entropy involved in the antiferromagnetic transition, calculated by integrating  $(C_0 - C_{70\text{ kOe}})/T$  over the transition region, is  $2.1\text{ J mol}^{-1}\text{ K}^{-1}$ . This value is surprisingly low, reaching only 9 % of the full entropy of  $2R\ln 4$  ( $23.05\text{ J}$

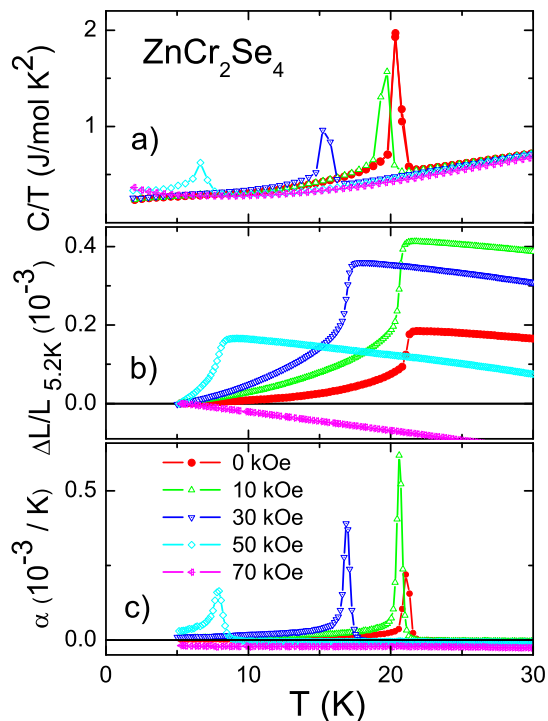


FIG. 2: (color online) Temperature dependence of the heat capacity plotted as  $C/T$  vs  $T$  (a), of the thermal expansion  $\Delta L/L$  (b) and of the thermal expansion coefficient  $\alpha$  (c) for a single crystalline ZnCr<sub>2</sub>Se<sub>4</sub> sample at different external magnetic fields between 0 and 70 kOe applied along  $\langle 001 \rangle$  axis.

mol<sup>-1</sup>K<sup>-1</sup>) expected for the complete ferromagnetic alignment of the Cr spins. Assuming that the magnon contribution to the specific heat for 0 and 70 kOe does not differ too much, this anomalously low transition entropy reveals that the main part of the total spin entropy is released already at temperatures much higher than  $T_N$ . This indicates strong spin fluctuations in the paramagnetic regime characteristic for highly frustrated magnets. Fig. 2a also documents how magnetic order can be fully suppressed by an external magnetic field yielding a quantum-critical point with a  $T = 0$  AFM phase transition. To our knowledge this is one of the rare examples how quantum criticality can be reached not only in metallic systems with competing magnetic and Kondo-type interactions but also in insulating geometrically frustrated magnets.

Figure 2b presents the thermal expansion  $\Delta L/L(T)$  for a single crystalline sample measured at different magnetic fields.  $\Delta L/L$  exhibits a strong drop at  $T_N$ . Figure 2c illustrates the respective variations of the thermal expansion coefficient  $\alpha = (1/L)dL/dT$ . It manifests a steep narrow maximum at  $T_N$  for zero-field which shifts to lower temperature and broadens with increasing field similarly to the anomaly in the specific heat. In contrast to the specific heat, the amplitude of the maximum in  $\alpha$  and the change of  $\Delta L/L$  at the transition temperature show a non-monotonous variation with magnetic field. It increases with the field up to the critical value  $H_{c1}$  of the metamagnetic transition and then decreases for higher

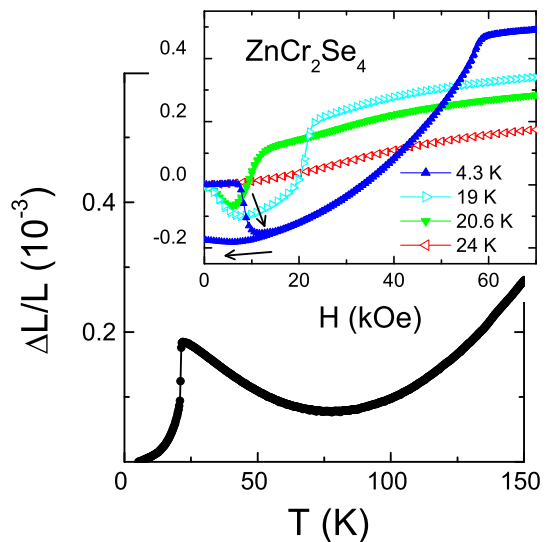


FIG. 3: (color online) Thermal expansion  $\Delta L/L(T)$  of a ZnCr<sub>2</sub>Se<sub>4</sub> single crystal for an extended temperature range illustrating the negative thermal expansion between  $T_N$  and 75 K. Inset:  $\Delta L/L(H)$  at several temperatures below and above  $T_N$ .

fields. Such a behavior for low fields can be attributed to the reorientation of magnetic domains with three different nearly equivalent  $\langle 001 \rangle$  axes being the spiral propagation direction in agreement with the magnetization measurements [20]. The thermal expansion is strongly anisotropic being nearly three times larger along the  $\langle 001 \rangle$  axis compared to the  $\langle 111 \rangle$  axis.

The other important feature of  $\Delta L/L$  is a strong negative thermal expansion observed below 75 K down to  $T_N$  as demonstrated in Figure 3. It is interesting to note that in an external field of 70 kOe a strictly constant negative thermal expansion evolves at the lowest temperature of our measurements (5.2 K), resulting in an approximately linear decrease of the cell dimension with increasing temperature up to 75 K (see Figs. 2b and 2c). Negative thermal expansion could result from the geometrical frustration of the lattice degree of freedom [21] and is usually explained by highly anharmonic vibrational modes [22], which in the case of ZnCr<sub>2</sub>Se<sub>4</sub> have to result from strong coupling of the phonons to the spin degree of freedom. The magnetostriction, i.e. the field dependence of the lattice expansion, below and above  $T_N$  is illustrated in the inset of Fig. 3. The monotonous increase of  $\Delta L/L(H)$  observed above  $T_N$  changes into an initial decrease up to the metamagnetic transition at 10 kOe followed by a stronger increase up to the saturation field at temperatures below  $T_N$ . Note the unusually high value of the magnetostriction which is comparable to that observed in giant magnetostrictive materials with strong spin-orbital coupling [23]. However, it is necessary to remind that a strong spin-orbital coupling is not expected here, as we additionally proved by the electron-spin resonance measurements discussed below.

To gain insights into the local magnetic properties of

ZnCr<sub>2</sub>Se<sub>4</sub> we measured the temperature dependence of the ESR absorption of the Cr spins which consists of a single exchange-narrowed Lorentz line in the paramagnetic regime. Figure 4 shows the temperature dependence of the resonance field and linewidth for the single crystalline sample in form of a disc with (110) plane orientation for temperatures 21 K <  $T$  < 300 K. From the resonance field we derived an asymptotic  $g$ -value of 1.996 at high temperatures close to the spin-only value in good agreement with the results of the paramagnetic susceptibility. This additionally indicates only minor spin-orbit coupling typical for Cr<sup>3+</sup> ions [24]. For lower temperatures and approaching the magnetic phase transition the resonance field strongly decreases as often observed close to the onset of AFM order due to the opening of the excitation gap. The  $T$ -dependence of the intensity at resonance absorption compares well with the bulk susceptibility indicating the same Curie-Weiss law at high temperatures (inset in Fig. 4a). The linewidth, which is a measure of the spin correlations, strongly increases when approaching the AFM ordering temperature. For an exchange coupled spin system outside the critical regime and above the phase transition, the temperature dependence of the linewidth should be proportional to the  $\Delta H_\infty / (T\chi)$  where  $\Delta H_\infty$  denotes the asymptotic high-temperature linewidth [25]. Deviations from this expected behavior indicated by the dashed line in Fig. 4b set in already below 200 K signaling significant spin fluctuations due to strong exchange interactions despite the low ordering temperature. This underlines the competition of the FM and AFM interactions evident from the corresponding high-temperature deviation of the susceptibility from the CW law. Note that no anisotropy of the spectra is visible in the paramagnetic regime. Below  $T_N$  a broad absorption band is observed centered on zero magnetic field. The angular dependence of the corresponding linewidth is shown in the inset of Fig. 4b. It reflects a cubic anisotropy with a maximum at  $\langle 111 \rangle$  and minima at  $\langle 110 \rangle$  and  $\langle 001 \rangle$  axes indicating strong coupling of the magnetization to the lattice in agreement with the earlier higher frequency ESR results [26].

The obtained data reveal a strong spin-lattice coupling and provide experimental evidence for a spin-driven origin of the structural transformation from the high-temperature cubic phase to a lower symmetry below the magnetic transition at  $T_N$ . The dominant magnetic coupling mechanism in ZnCr<sub>2</sub>Se<sub>4</sub> is superexchange which includes  $nm$  FM Cr-Se-Cr and  $nmn$  AFM Cr-Se-Zn-Se-Cr or Cr-Se-Se-Cr exchange interactions [19]. These competing exchange interactions establish the complex incommensurate spin order in this compound. The FM 90° Cr-Se-Cr exchange governs the ferromagnetic order in the (001) planes. The AFM exchange is probably responsible for the spin arrangement between the adjacent (001) planes. An external magnetic field changes the balance between FM and AFM interactions enhancing the ferromagnetic correlations and thus reduces the angle between the spins in the adjacent FM planes. In agreement with our observation of the concomitant reduction of the anomalies of specific heat and thermal expansion by an external magnetic field this cor-

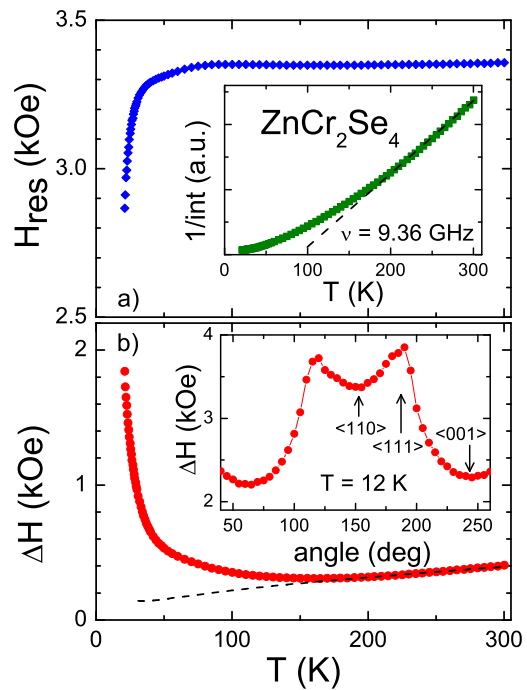


FIG. 4: (color online) Temperature dependence of the resonance field (a) and linewidth (b) for a single crystalline ZnCr<sub>2</sub>Se<sub>4</sub> disc with (110) plane orientation. The dashed line indicates the expected behavior for an exchange coupled system. Upper inset: inverse intensity of the ESR line vs  $T$  showing a Curie-Weiss dependence at high temperatures. Lower inset: angular dependence of the linewidth at 12 K revealing magnetocrystalline anisotropy.

roborates the interpretation of the low-temperature structural symmetry breaking in ZnCr<sub>2</sub>Se<sub>4</sub> as due to bond frustration caused by competing exchange. This results in an extremely large influence of the magnetic field on the structural transition. The negative thermal expansion indicates a high degree of frustration of this highly symmetric lattice in the paramagnetic regime. This frustrated lattice is strongly receptive to weak perturbations which are primarily induced by magnetic order at  $T_N$ . The coupling between the magnetism and lattice may be realized via an exchange-striction mechanism similar to a spin-Peierls transition. However, compared to the 3D spin Jahn-Teller transition in chromium oxide spinels [9, 10, 11] and to the 1D spin-Peierls transition in CuGeO<sub>3</sub> [27] we observed a much stronger effect of an external magnetic field on the structural transition which we attribute to the strong bond frustration.

In conclusion, we investigated the bond frustrated AFM spinel ZnCr<sub>2</sub>Se<sub>4</sub> and found pronounced anomalies in the specific heat and thermal expansion at the onset of the antiferromagnetic helical order at the Néel temperature. Our results reveal strong spin-phonon coupling that generates the low-temperature structural instability in this compound. The observed negative thermal expansion is suggested to result from the high frustration of the lattice degrees of freedom. A colossal magnetostriction comparable to giant magnetostric-

tive materials is found despite the absence of strong spin-orbital coupling of the half-filled  $\text{Cr}^{3+} t_{2g}$  electronic state. An extremely strong suppression of the anomalies in the specific heat and thermal expansion by magnetic fields suggests a spin-driven origin of the structural transformation and proximity to a quantum critical point.

We are grateful to Dana Vieweg and Thomas Wiedenmann for experimental assistance. This work was supported by BMBF via VDI/EKM, FKZ 13N6917-B and by DFG within SFB 484 (Augsburg).

---

\* Corresponding author

- [1] S. Kondo *et al.*, Phys. Rev. Lett. **78**, 3729 (1997); A. Krimmel *et al.*, Phys. Rev. Lett. **82**, 2919 (1999).
- [2] S.-H. Lee *et al.*, Nature (London) **418**, 856 (2002).
- [3] P. G. Radaelli *et al.*, Nature (London) **416**, 155 (2002).
- [4] M. Schmidt *et al.*, Phys. Rev. Lett. **92**, 056402 (2004).
- [5] V. Fritsch *et al.*, Phys. Rev. Lett. **92**, 116401 (2004); A. Krimmel *et al.*, Phys. Rev. Lett. **94**, 237402 (2005).
- [6] R. Fichtl *et al.*, Phys. Rev. Lett. **94**, 027601 (2005).
- [7] J. Hemberger *et al.*, Nature (London) **434**, 364 (2005); S. Weber *et al.*, Phys. Rev. Lett. **96**, 157202 (2006).
- [8] Y. Yamasaki *et al.*, Phys. Rev. Lett. **96**, 207204 (2006).
- [9] S.-H. Lee *et al.*, Phys. Rev. Lett. **84**, 3718 (2000).
- [10] O. Tchernyshyov *et al.*, Phys. Rev. Lett. **88**, 067203 (2002).
- [11] Y. Yamashita and K. Ueda, Phys. Rev. Lett. **85**, 4960 (2000).
- [12] J. Hemberger *et al.*, Phys. Rev. Lett., in press.
- [13] F.K. Lotgering, Proc. Int. Conf. Magnetism, Nottingham, 1964 (The Institute of Physics and the Physical Society, London, 1965), p. 533 (1965).
- [14] R. Plumier, J. Physique **27**, 213 (1966).
- [15] R. Kleinberger and R. de Kouchkovsky, C.R. Acad. Sci. Paris **262**, 628 (1966).
- [16] M. Hidaka *et al.*, phys. stat. sol. (b) **236**, 570 (2003); M. Hidaka *et al.*, phys. stat. sol. (b) **236**, 9 (2003).
- [17] J. B. Goodenough, Phys. Rev. B **117**, 1442 (1960).
- [18] M. Hamedoun *et al.*, J. Phys. C **19**, 1783 (1986).
- [19] N. Menyuk *et al.*, J. Appl. Phys. **37**, 1387 (1966), K. Baltzer *et al.*, Phys. Rev. **151**, 367 (1966).
- [20] M. Nogués *et al.*, phys. stat. sol. (a) **91**, 597 (1985).
- [21] A.P. Ramirez, Nature (London) **421**, 483 (2003).
- [22] G. Ernst *et al.*, Nature (London) **396**, 147 (1998).
- [23] R. Mahendiran *et al.*, Appl. Phys. Lett. **82**, 242 (2003).
- [24] A. Abragam and B. Bleaney, *Electron Paramagnetic Resonance of Transition Ions*, Dover Publ.Inc., New York, 1986).
- [25] D.L. Huber *et al.*, Phys. Rev. B **60**, 12155 (1999).
- [26] K. Siratori *et al.*, J. Phys. Soc. Japan. **30**, 707 (1971).
- [27] M. Hase *et al.*, Phys. Rev. Lett. **70**, 3651 (1993); R.M. Eremina *et al.*, Phys. Rev. B **68**, 0144179 (2003).